Desalination and Water Treatment
www.deswater.com

doi:10.5004/dwt.2018.22141

107 (2018) 207–217
March

Comparison of cesium adsorption behavior of CHCF-PAN, MnO_2-PAN, STS-PAN, CM-PAN and AMP–PAN synthesized composites from aqueous solution

R. Saberi*, Y. Es-hagh, S. Azad, A. Rajabi

Nuclear Science and Technology Research Institute (NSTRI), PO Box 11365-8486, Tehran, Iran, Tel. +989121307069, email: rsaberi@aeoi.org.ir (R. Saberi), y.eshagh@ce.iut.ac.ir (Y. Es-hagh), soheil.azad89@gmail.com (S. Azad), a.rajabi@mi.iut.ac.ir (A. Rajabi)

Received 18 September 2017; Accepted 28 February 2018

ABSTRACT

In this manuscript, five organic–inorganic composite ion exchangers (CHCF-PAN, MnO_2-PAN, STS-PAN, CM-PAN and AMP–PAN) were synthesized and efficiency of cesium adsorption from aqueous solutions was compared. The synthesized composites were characterized by various techniques including XRD, FT-IR, TGA, SEM, BET, XRF, CHN elemental analysis. In order to obtain the optimum conditions for the Cs^+ adsorption, the influence of pH, contact time, temperature and presence of the interfering cations on the distribution coefficient of cesium onto composite sorbents were studied. Also, adsorption thermodynamic parameters were determined and it was observed that the adsorption of cesium on the adsorbent is an endothermic and spontaneous process. The Langmuir and Freundlich isotherm models were fitted to the obtained experimental sorption data. Also, the adsorption dynamic capacities of the synthesized composites in a fixed bed column were evaluated. Finally, it was concluded that synthesized AMP-PAN composite gave high efficiency of cesium removal from aqueous solutions, which was 67.77%.

Keywords: Synthesized composite sorbents; Ion exchange; Cesium adsorption; Fixed bed

1. Introduction

The removal of radioactive pollutants from contaminated water has recently become one of the most important processes because of which its importance is becoming more profound with increasing nuclear facilities. Among all the radioactive elements, gamma ray emitters ^{134}Cs and ^{137}Cs are the most powerful and most hazardous nuclear fission products of uranium [1,2]. Both isotopes are considerably been harmful to human and can easily destroy the environmental habitat since they can quickly cause its migration through ground and sea waters, accumulating in the biosphere for hundreds of years [3,4].

Several methods have been developed to eliminate radio cesium from contaminated water. [5–14]. Among the methods, ion exchange process has recently attracted a lot of preferences such as convenience, efficiency and selectivity. Use of different materials has been previously reported for this technique[10–13].

It was found that the inorganic ion exchangers such as zeo lites, multivalent phosphates, hexacyanoferrates, silicotitanates, clay minerals, and metal oxides have several superior qualities required for the treatment of waste streams compared to organic materials [11,14–20]. However, the slow mass-transfer rate in column operation has been the impeding factor for extensive operations [21]. For solving this problem, composite ion exchangers have been widely studied for treatment of liquid wastes. Composite ion exchangers have been recently used for their better selectivity for some metal ions sorption, increased mechanical and chemical resistance, lower solubility in aqueous solution and better kinetics of exchange relative to pure inorganic exchangers [22]. In composite ion exchanger, inorganic materials are active components to which all the radio nuclides are bound and organic materials are simply inert binders.

Polyacrylonitrile (PAN) is one of the most favorable organic binders, due to its characteristic such as excellent

*Corresponding author.

pelletizing property, good solubility for organic solvents, chemical stability and strong adhesive forces with inorganic materials [23]. PAN beads are highly porous and can accommodate very high loadings of ion exchange material (5–95%) into the PAN matrix. These highly porous PAN beads demonstrate a number of advantages over other granular sorbents [24].

Someda et al. used [25] Zn and Cu hexacyanocobaltateson PAN for removal of the radioactive cesium from different aqueous solutions. Milonji et al. [26] used copper hexacyanoferrate/polymer/silica composites for the cesium sorption from aqueous solution in batch and dynamic conditions. Younjin Park et al. [10] developed that the AMP at a loading of 50 wt% provided on SBA-15 showed a high ion exchange capacity with the negligible influence of coexisting cations and acidity for Cs ion sorption in the batch tests. Chunyan Sun et al. [27] showed that the AMP/Al-MCM-41 adsorbs up to 84% of the Cs^+ ions in the concentration range tested.

In this study, five synthesized composite ion exchangers which include: Copper Hexa Cyano Ferrate (ii)-PAN (CHCF-PAN), MnO_2-PAN, Sodium Titano Silicate-PAN (STS-PAN), Cerium Molybdate-PAN (CM-PAN) and Ammonium Molybdo Phosphate-PAN (AMP–PAN) are used for the removal of cesium from aqueous solution are studied. Many factors such as adsorption kinetics, isotherm models, thermodynamic parameters, as well as the influence of pH, interfering cations, temperature, and contact time on adsorption are investigated. In addition, the dynamic studies were carried out to obtain the dynamic capacities of the synthesized adsorbents. Finally, the composite adsorbent with highest capability is introduced for using in adsorption column.

2. Experimental

2.1. Reagents and apparatus

All the chemicals used in this work were of analytical grade. Potassium hexacyanoferrate, ammonium cerium (IV) nitrate, ammonium molybdate tetrahydrate, tetraethyl orthosilicat, tetraethyl orthotitanate, copper (II) nitrate trihydrate, manganese (II) sulfate monohydrate, ammonium nitrate, potassium permanganate, dimethyl sulfoxide (DMSO), sulfuric acid, phosphoric acid, sodium hydroxide, ceasium chloride were purchased from Merck (Darmastdt, Germany).nitric acid and hydrochloric acid were supplied by Fluka. polyacrylonitrile (PAN) was obtained from Aldrich. The stock solutions of chemicals were prepared by dissolving CsCl in distilled water.

Various apparatuses were used to characterize the synthesized composite Sorbents. X-ray powder diffractometry was carried out using an 1800 PW Philips diffractometer in order to determine the structure of the adsorbers; The amounts of synthesized composite elements were determined by the X-ray Fluorescence Unit (Oxford ED 2000) and the infrared spectra were recorded using a Brucker-Vector 22 spectrophotometer (Brucker, Germany); The amount of Na^+, K^+, Ca^{2+} and Mg^{2+} cations was measured by a Perkin Elmer Atomic Adsorption Spectrometer (AAS) model 843; Brunauer-Emmett-Teller (BET) specific surface area was specified through nitrogen adsorption isotherms using Quantachrome NOVA2200e system; Carbon, Hydrogen and Nitrogen contents of the composites were determined using an Elementar-Vario EL III, CHN elemental analyzer; Scanning electron microscope (SEM) imaging was performed by means of a Philips XL-30; Thermogravimetry–differential scanning calorimetry (TGA) was carried out using a DuPont model 951. The radioactivity was counted using a high purity germanium detector gamma spectrometer Ortec model GMX-15185-5 and finally the pH measurement was made with a Schott pH-meter model CG841.

2.2. Preparation of composite sorbents

2.2.1. Synthesize of CHCF–PAN composite solution

For preparation of CHCF, 0.25 mol/L $K_4[Fe(CN)_6]$ was mixed with 0.75 mol/L $Cu(NO_3)_2.3H_2O$ with the volume ratio of 1:1 at 50ºC and 500 rpm. After 48 h, the brown sediment was filtered and washed with distilled water, then dried at 70ºC for 24 h. Finally, the precipitate powdered by a mill and sieved to size of 224–400 μm.

For preparation of CHCF–PAN composite solution, 5 g of PAN, 55 mL of DMSO, and a few drops of Tween-80 were stirred for 3 h in a three-necked flask. Then, 5 g of CHCF powder and 20 mL of DMSO which were mixed at 50ºC for 2 h, added to the above solution. Finally, a homogeneous solution of composite dope was prepared by stirring at 50ºC for 3 h [15].

2.2.2. Synthesize of MnO_2–PAN composite solution

For preparation of MnO_2, 500 mL of 1 mol/L $MnSO_4{\cdot}H_2O$ solution containing 1 mol/L H_2SO_4 was added to 250 mL of 1.5 mol/L $KMnO_4$ solution containing 1 mol/L H_2SO_4 and mixed in a three-necked flask for about 4 h at 60°C. After 2 d the precipitate was filtered and washed with 300 ml of 6 mol/LHNO_3, and dried at 60°C for 24 h (repeated over 5 times).

For preparation of MnO_2-PAN composite solution, 3.2 g of PAN, 40 mL of DMSO, and a few drops of Tween-80 were stirred for 2 h in a three-necked flask. Then, 4 g of MnO_2 powder and 10 mL of DMSO which were mixed at 50°C for 1 h, added to the above solution. Finally, a homogeneous solution of composite dope was prepared by stirring at 50°C for 4 h. [28]

2.2.3. Synthesize of STS-PAN composite solution

For preparation of STS, 39 mL of 6 mol/L NaOH solution was added to 6.8 g of $TiC_8H_{20}O_4$ 97% and 5.0 g of $SiC_8H_{20}O_4$ 99%. The synthesized precipitates were carried out under hydrothermal conditions at temperature 150°C for 5 d.

For preparation of STS-PAN composite solution, 2.4 g of PAN, 25 mL of DMSO, and a few drops of Tween-80 were stirred for 4 h in a three-necked flask. Then, 3 g of STS powder and 25 mL of DMSO which were mixed at 50°C for 3 h, added to the above solution. Finally, a homogeneous solution of composite dope was prepared by stirring at 50°C for 4 h. [21]

2.2.4. Synthesize of CM–PAN composite solution

For preparation of CM, 250 mL of 0.5 mol/L $(NH_4)_2Ce(NO_3)_6$ and 250 mL of 1 mol/L$(NH_4)_6Mo_7O_{24}{\cdot}4H_2O$

were mixed in a three-necked flask for about 4 h at 50°C, by the gradual addition of 6 mol/L HNO_3 to the solution were obtained a yellow precipitates. The resulting precipitate was filtered and washed with distilled water and dried at 50°C, then sieved to size of 224–400 μm.

For preparation of CM–PAN composite solution, 5 g of the synthesized CM powder was mixed with 10 mL of DMSO and stirred continuously in a three-necked flask for 3 h at 50°C. 4 g of PAN were then mixed with 40 mL of DMSO solution and a few drops of Tween-80 surfactant was added and stirred for 4 h at 50°C [29].

2.2.5. Synthesize of AMP-PAN composite solution

For preparation of AMP, 100 mL of 0.5 mol/L NH_4NO_3, 50 mL of 2 mol/L H_3PO_4 and 50 mL of 2 mol/L $(NH_4)_6Mo_7O_{24}{\cdot}4H_2O$ were mixed in a three-necked flask for about 4 h at 25°C, by the gradual addition of 6 mol/L HNO_3 to the solution were obtained a yellow precipitates.

For preparation of AMP-PAN composite solution, 3.2 g of PAN, 32 mL of DMSO, and a few drops of Tween-80 were stirred for 4 h in a three-necked flask. Then, 4 g of AMP powder and 8 mL of DMSO which were mixed at 50°C for 3 h, added to the above solution. Finally, a homogeneous solution of composite dope was prepared by stirring at 50°C for 4 h [30].

2.2.6. Preparation of composite granules

To synthesize spherical and homogeneous composite granules, the dissolved air in the composite dope was removed by vacuum pump, and the air-free composite dope was passed through inside a dual nozzle while the compressed air was ejected through the outside annulus of the dual nozzle to adjust the size of the composite granules [31]. The composite solution and an aqueous solution, which was put underneath a nozzle and used as a medium for trickling the composite granules in it, were stirred by magnetic stirrers. A small amount of a surfactant was added to the aqueous solution in order to decrease the water adhesion and to obtain spherical and tailless granules [30]. The composite granules were ejected through the dual nozzle and then dropped in distilled water, which was used as a gelation agent. Finally, the granules were washed using demineralized water and dried at 50°C for 2 d. The bead sizes were varied in the range of 2–3 mm with the air pressure variation.

2.3. Experimental procedure

The distribution coefficient (K_d) of cesium on composite adsorbents was studied at various contact times, temperatures, pHs, and interfering cations by equilibrating 0.1 g of the prepared composites with 10 mL of the labeled 10^{-4} mol/L cesium solution.

For the evaluation of K_d as a function of contact time, from 5–120 min time intervals were applied. K_d was calculated using the following equation:

$$K_d = \frac{C_0 - C_e}{C_e} \times \frac{V}{m} \quad (1)$$

where C_0 and C_e are introduced as the initial and final concentration of the aliquots (mmol/L), respectively. V (mL) is the volume of the solution and m (g) is the mass of sorbent.

Batch adsorption experiments were carried out at ambient temperature except for the temperature dependence studies where the temperature was varied from 25 to 65°C.

The suitable pH was adjusted with NaOH and HCl. The same experimental conditions were applied in order to investigate the influence of Na^+, K^+, Ca^{2+} and Mg^{2+} cations on the K_d of cesium. The sorption isotherm experiments were conducted at 25°C and suitable pH by batch sorption procedure.

After obtaining the optimum conditions for adsorption of Cs^+ in batch process, the application of the composite sorbents was evaluated in continuous column system. Its application was investigated for a continuous system by passing the aqueous solution with flow rate of 0.66 mL/min into an ion exchange column with radius of 0.8 cm and length of 60 cm that packed with 0.2 g of the composite sorbent. The adsorbent bed volume was equal 120.6 cm^3 and the flow rate of the aqueous solution was 15 BV/hr.

3. Results and discussion

3.1. Characterization of synthesized composites

By analyzing the XRD patterns of the synthesized composites, it was observed that the XRD data of the synthetic inorganic sorbents are in good agreement with the XRD pattern showed in Fig. 1. Furthermore, there are no diffraction peaks in the XRD pattern of PAN indicating its amorphous structure, but the 2θ values at the peak points of synthesized composite sorbents are the same as those in synthetic inorganic sorbents, it can be deduced that their crystalline structures are very similar [30,21,28,15], except for the CM–PAN composite where exist as amorphous substances, as identified by the absence of any sharp diffraction peak along the XRD pattern [29]. Using the above facts, it was determined that synthesized sorbents composition has been accurately synthesized.

By comparison between the IR spectrum of synthetic inorganic sorbents and synthesized composite, it can be concluded that there are some similar adsorption peaks in both spectra. For example, an IR spectrum of the synthesized CHCF and CHCF–PAN composite is shown in Fig. 2. The presence of carbon-metal bond in the structure of CHCF and CHCF–PAN is determined by the adsorption peak in the region of 450–600 cm^{-1}. The sharp and strong peaks at 2096 cm^{-1} in CHCF and CHCF–PAN spectra are due to the stretching vibration of C≡N. The bending vibration of water molecules in both materials is specified by the peak at 1615 cm^{-1} and finally the adsorption peaks at 3421 and 3265 $cm^{-1}$are attributed to the stretching vibration of interstitial water [15]. Other IR spectrums of synthesized composite sorbents are provided in the previous literatures. [21,28–30].

The gamma irradiation of the synthesized composite was carried out, using ^{60}Co as a source, at a dose rate of 0.38 Gy s^{-1}. IR spectrums of synthesized composite prior to and after gamma irradiation (100 and 200 kGy doses) were investigated. It can be seen in Fig. 3, all of synthesized composite ion exchangers were resistant to gamma irradiation of up to 200 kGy.

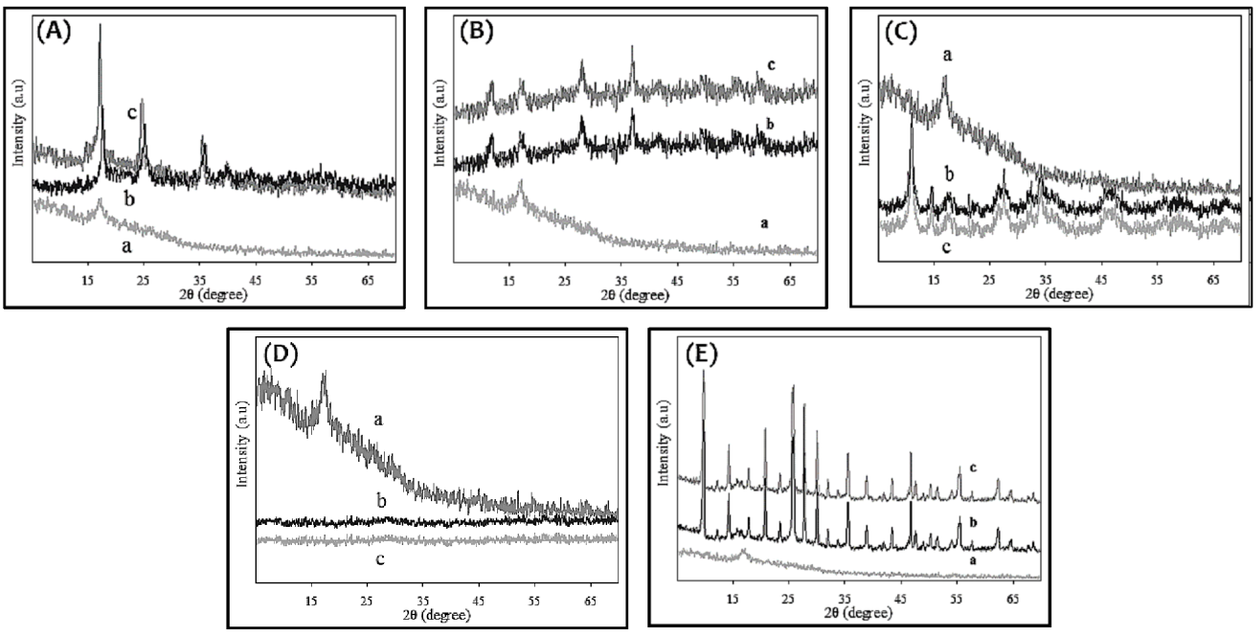

Fig. 1. XRD patterns of (a) PAN, (b) component and (c) components–PAN composite. (A) CHCF-PAN, (B) MnO2-PAN, (C) STS-PAN, (D) CM-PAN and (E) AMP-PAN.

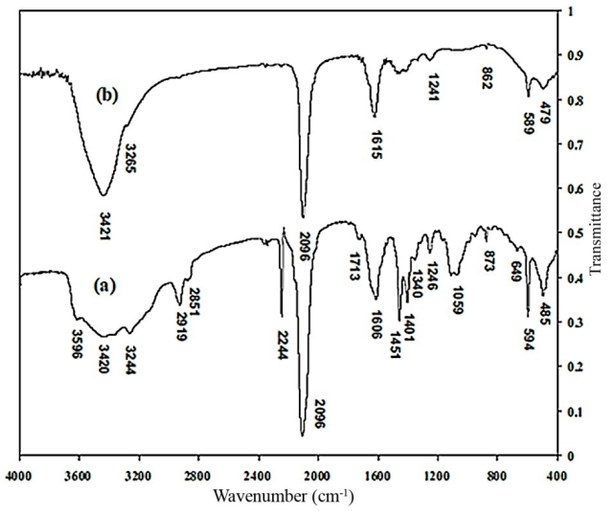

Fig. 2. FT-IR spectra of (a) CHCF–PAN composite and (b) CHCF.

The BET surface area of synthesized composite sorbents was showed in Table 1. It is interesting that some of the BET surface area values, such as AMP–PAN composite which is more than twice the corresponding value (32.69 m^2/g) synthesized by Park et al [37].

SEM imaging of synthesized composite beads are shown in Fig. 4. SEM photographs were obtained by accelerating electrons within a range of 1–30 KeV. It was found from Fig. 4-(A) that the internal structure of CHCF-PAN composite granules is very porous. The pores size of the granules in their inner part was larger than that near the surface. The dispersion of CHCF, throughout the binding matrix of the composite is a sign of being an effective ion exchanger for cesium adsorption from aqueous solution [15]. The SEM photograph of MnO_2–PAN in Fig. 4B was revealed that the particles were not homogeneous. The kinetic of sorption on these adsorber beads must be very fast, since the active material, is found to be dispersed throughout the binding matrix [28]. Fig. 4C indicates that the structure of synthesized STS-PAN is tunnel-shaped with a high adsorption level [21]. Figs. 4D and 4E show that the internal structure of the composite granules is very porous which helps cesium adsorption from the aqueous solution [29,30].

Table 1
BET surface area of synthesized composite sorbents

Composite sorbent	BET surface area (m^2/g)	BET pore size (Å)	BET pore volume (cm^3/g)
CHCF-PAN	73.58	463.4	0.247
MnO_2-PAN	53.03	334.5	0.167
STS-PAN	96.66	588.3	0.315
CM-PAN	25.18	163.4	0.091
AMP-PAN	75.90	471.1	0.255

The obtained results from CHN elemental analyzer and XRF spectroscopy unitare shown in Table 2 [15,21,28,29,30].

In order to study the stability of the synthesized composite adsorbents against thermal conditions, the TGA thermal analysis was carried out in the temperature range of 25 and 800°C, which indicates the decomposition steps

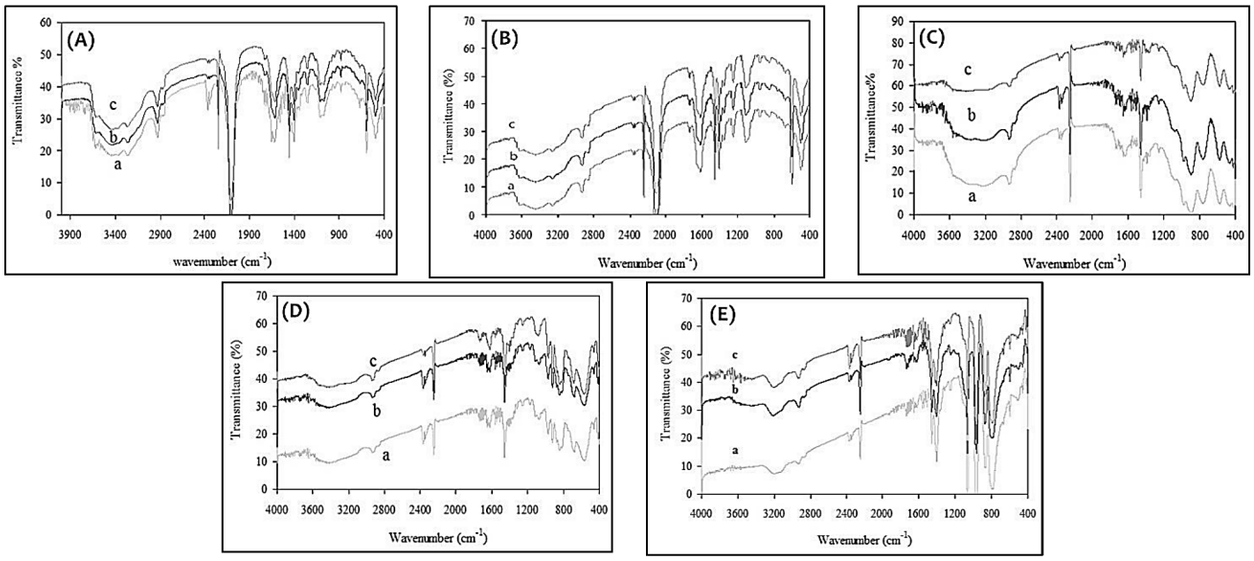

Fig. 3. IR spectra comparison over modes of (a) unirradiated (b) irradiated up to 100 KGy and (c) irradiated up to 200 KGy. (A) CHCF-PAN, (B) MnO_2-PAN, (C) STS-PAN, (D) CM-PAN and (E) AMP-PAN.

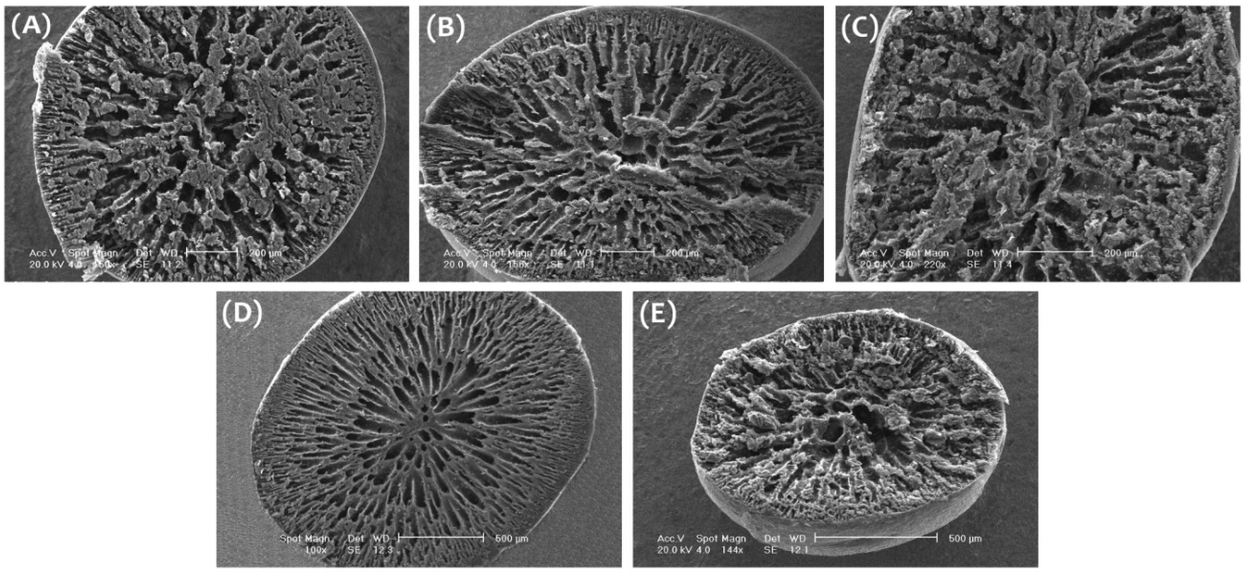

Fig. 4. Scanning electron microscopic photograph of composite absorber bead cross-section. (A) CHCF-PAN, (B) MnO_2-PAN, (C) STS-PAN, (D) CM-PAN and (E) AMP-PAN.

(Fig. 5). The results obtained for AMP-PAN shows that the weight reduction up to 190ºC and from 190–450ºC is due to elimination of free water molecules and release of the interstitial water molecules, respectively. Also, the structural collapse of polymer present from 190–450ºC in the AMP-PAN composite. The weight reduction in 450–800°C is attributed to release of ammonia and hydrogen cyanide gases from the composite and formation of molybdenum oxide. Therefore, AMP–PAN ion exchanger composite is stable up to 190°C. [30] Similarly, for other synthesized composite sorbents, TGA results showed that the CHCF–PAN,MnO_2–PAN, STS-PAN, and CM–PAN composites are stable up to 200, 310, 275, and 300°C, respectively [15,21,28,29].

3.2. Kinetic studies

3.2.1. Effect of pH

In order to determine the optimum chemical conditions, Cs^+ adsorption was investigated at various pH values from 1.0 to 9.0. As it can be seen in Fig. 6, the adsorption

Table 2
Elemental analysis results of the synthesized composite sorbents

Element	Weight (%)				
	CHCF-PAN	MnO_2-PAN	STS-PAN	CM-PAN	AMP-PAN
Fe	5.10				
Cu	5.80				
Mn		41.31			
Ti			34.50		
Si			13.60		
Ce				4.7	
Mo				10.0	6.0
P					1.7
C	39.06	29.1	32.78	36.07	44.24
H	4.42	3.03	3.78	3.64	4.13
N	19.80	10.60	6.54	13.72	17.8

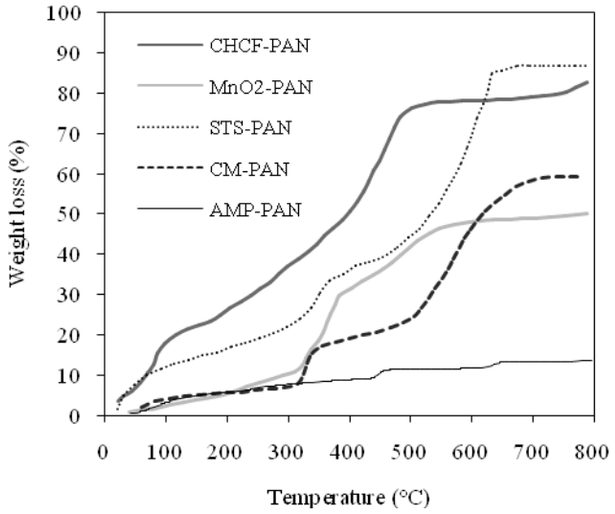

Fig. 5. TGA curves of the synthesized composite sorbents.

process is continuously improved by increasing pH value from acidic to alkali medium. Low distribution coefficient in acidic environments can be attributed to competition of H^+ with Cs^+ cations for the exchange sites in the adsorbent. All sorption experiments in the present study were carried out at pH equal 7 [20].

3.2.2. Effect of contact time

The adsorption of Cs^+ increases with time until reaching equilibrium between two phases. Fig. 7 shows that the equilibrium times between aqueous solution and CHCF–PAN, MnO_2–PAN, STS-PAN, CM–PAN and AMP-PAN composites are 280, 35, 130, 30 and 35 min, respectively.

3.2.3. Effect of temperature

The results of solution temperature effect on K_d of Cs^+ are shown in Table 3. It can be seen, by enhancing the solution temperature, the distribution coefficient value of cesium increases.

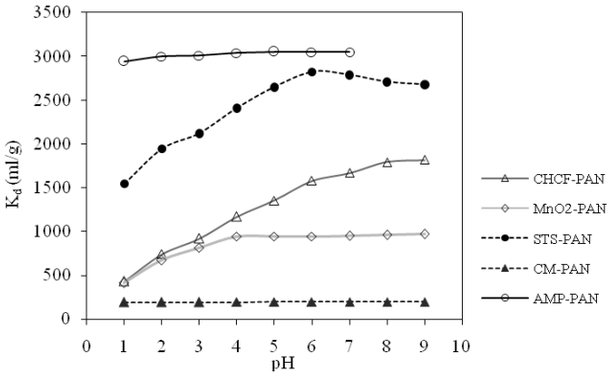

Fig. 6. Variation of cesium distribution coefficient with pH.

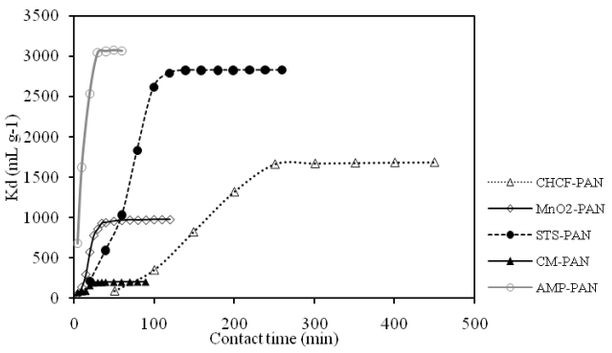

Fig. 7. Variation of cesium distribution coefficient with contact time.

3.2.4. Effect of interfering ions

Change of distribution coefficient values of Cs^+ along with the tracer was evaluated in the presence of Na^+, K^+, Ca^{2+} and Mg^{2+} cations at 10^{-4} mol/L concentration added

Table 3
The effect of solution temperature on the cesium distribution coefficient

Temperature (K)	K_d (*mL/g*)				
	CHCF-PAN	MnO_2-PAN	STS-PAN	CM-PAN	AMP-PAN
298	1673	944	2802	197	3055
308	1820	983.4	2883	201	3120
318	1927	1012.5	2984	205	3168
328	2056	1041.8	3267	208	3208
338	2109	1058.5	3454	211	3278

Table 4
The effect of interfering ions in the solution on the cesium distribution coefficient

Interfering ion	K_d (*mL/g*)				
	CHCF-PAN	MnO_2-PAN	STS-PAN	CM-PAN	AMP-PAN
None	1673	944	2802	197	3055
Na^+	229	411.9	612	66	856
K^+	167	257.2	429	38	826
Ca^{2+}	535	71.4	802	91	1023
Mg^{2+}	319	132.8	907	82	1018

Table 5
Thermodynamic parameters for cesium adsorption on the synthesized composite sorbents

Synthesized composite	$\Delta H°$ (*kJ/mol*)	$\Delta S°$ (*kJ/mol·K*)	$-\Delta G°$ (*kJ/mol*)				
			298 K	308 K	318 K	328 K	338 K
CHCF-PAN	4.9248	0.07833	18.4176	19.2009	19.9842	20.7675	21.5508
MnO_2-PAN	2.417	0.065	16.953	17.603	18.253	18.903	19.553
STS-PAN	4.5177	0.0809	19.6165	20.4264	21.2363	22.0462	22.856
CM-PAN	1.4398	0.0487	13.0921	13.5798	14.0774	14.5551	15.0427
AMP-PAN	1.4406	0.07154	19.8801	20.5956	21.311	22.0265	22.7419

in the form of their nitrates at 298 *K*. The results (Table 4) indicate that the distribution coefficient of cesium has decreased in the presence of interfering ions. The apparent influences of added cations on the adsorption of Cs^+ can be attributed to their similar chemical characteristics or other factors [38].

3.3. Adsorption thermodynamic parameters

In order to obtain the thermodynamic nature of the sorption process, several adsorption thermodynamic parameters including standard enthalpy ($\Delta H°$), standard entropy ($\Delta S°$), and standard Gibbs free energy ($\Delta G°$) were determined. The amounts of $\Delta H°$ and $\Delta S°$ were calculated from the slope and intercept of the straight line obtained from plotting ln K_d values versus reciprocal temperature, respectively, from the following equation: [39]

$$lnK_d = \Delta S°/R - \Delta H°/RT \quad (2)$$

After calculating $\Delta H°$ and $\Delta S°$, $\Delta G°$ of adsorption was calculated from the equation below:

$$\Delta G° = \Delta H° - T\Delta S° \quad (3)$$

The values of $\Delta H°$, $\Delta S°$ and $\Delta G°$ are presented in Table 5. The positive amount of $\Delta H°$ and the negative amounts of $\Delta G°$ at different temperatures reveal that the adsorption of cesium on the synthesized composites is an endothermic and a spontaneous process.

3.4. Adsorption isotherms

Sorption isotherm models are usually used to obtain the relationship between the concentration of dissolved adsorbate in the aqueous solution and the amount of adsorbate on the solid phase at a constant temperature and pH [40]. The adsorption isotherm parameters show actually the surface properties and affinity of the sorbent. The Langmuir, Freundlich, Dubinin–Radushkevich (D–R), Redlich-Peterson, Radke-Prausnitz and Brunauer-Emmett-Teller (BET) isotherms are common kinds of several isotherm models [15]. In this paper Langmuir and Freundlich models are applied to calculate the sorption data of Cs^+ on synthesized composite adsorbents.

The experimental sorption isotherm of the prepared composite ion exchangers. Under optimum condition for each experiment, the maximum Cs adsorption value were 0.059, 0.0545, 0.075, 0.0445 and 0.079 (mmol/g) for CHCF–PAN, MnO_2–PAN, STS-PAN, CM–PAN and AMP-PAN composites, respectively, at the equilibrium concentration of 10 mmol/L.

3.4.1. Langmuir isotherm

The Langmuir sorption isotherm has been widely used to characterize the adsorption phenomena from solution. It is valid for homogeneous and mono layer adsorption onto a surface with a finite number of identical sites, each of which can only hold one molecule and there is no transmigration of adsorbate in the plane of the surface. The form of Langmuir isotherm can be represented by the following equation [41]:

$$\frac{C_e}{q_e} = \frac{C_e}{q_{\max}} + \frac{1}{q_{\max} b} \tag{4}$$

where q_{max} (mmol/g) is the maximum adsorption at monolayer, C_e (mmol/L) is the equilibrium concentration of Cs^+ in solution, q_e (mmol/g) is the amount of metal ions per unit weight of adsorbent at equilibrium and b (L/mmol) is the Langmuir constant related to the affinity of binding sites, which is a measure of the energy of adsorption. With the slope and intercept of the linearized plot of C_e/q_e versus C_e, q_{max} and b can be calculated.

3.4.2. Freundlich isotherm

The Freundlich isotherm is an empirical equation that en compasses the heterogeneity of sites and the exponential distribution of sites and their energies. Also, Freundlich isotherm model stipulate that the ratio of solute adsorbed to the solute concentration is a function of the solution. This model allows for several kinds of sorption sites on the solid and represents properly the sorption data at low and intermediate concentrations on heterogeneous surfaces. The logarithmic form of the model has the following form [42]:

$$\log q_e = \log K_F + \frac{1}{n} \log C_e \tag{5}$$

where K_F and n are Freundlich constants related to the adsorption capacity and adsorption intensity, respectively. Values of K_F and $n$are calculated from the slope and intercept of the linear plot of $log\ q_e$ against $log\ C_e$.

According to the value of correlation coefficients (R^2) in Table 6, it can be concluded that the cesium adsorption on the synthesized STS-PAN and AMP-PAN composites is mono layer and the Langmuir model fits the adsorption data better than the Freundlich model. But adsorption of Cs^+ ions into the CHCF-PAN, MnO_2-PAN and CM-PAN composites correlates well with the Freundlich model. It is important to note that the applicability of Freundlich to the studied sorption process shows that heterogeneous energetic distribution of active sites on the surface of the sorbent is possible [29].

3.5. Dynamic studies

The experimental conditions of continues adsorption is difference with the batch experimental conditions, because the adsorption in continuous systems does not reach equilibrium and the flow does not have adequate time to exchange all the metal ions with the sorbent. Therefore, The sorption capacity in column systems is decreased in comparison with batch systems, and it is necessary to provided dynamic study to obtain parameters such as, dynamic sorption capacity and dynamic sorption efficiency from the breakthrough curve. Further more the volume of solution passing through the adsorbing column is 200 cc, the amount of all adsorbing sorbents equal to 0.2 g, temperature of solutions 298 K and contact time is 60 min. Synthesized adsorbents at different pH have different efficiencies, but to compare these absorbers in the same conditions, pH of all solutions was assumed equal to 7. Fixed bed column adsorption experiments were carried out to study the adsorption dynamics. The shape of the breakthrough curve and the time for the breakthrough appearance are the two main factors for determining the operation and the dynamic response of the sorption column. The position of the breakthrough curve along the volume/time axis depends on the capacity of the column with respect to bed height, the feed concentration and flow rate [14].

In column fixed bed adsorption, the concentrations in the fluid phase and the solid phase change with time as well as with position in the bed. At first time, most of the mass transfer takes place near the inlet of the bed, where the fluid contact fresh adsorbent. After a few minutes, the solid near the inlet is nearly saturated, and most of mass transfer takes place further from the inlet [21].

Table 6
The parameters of Langmuir and Freundlich isotherms at 298 K

Synthesized composite	Langmuir constants			Freundlich constants		
	q_{max} (mmol g^{-1})	b (L $mmol^{-1}$)	R^2	K_F (mmol g^{-1})	$1/n$	R^2
CHCF-PAN	0.192	0.044	0.991	0.084	0.862	0.998
MnO_2-PAN	0.242	0.030	0.914	0.007	0.909	0.996
STS-PAN	0.440	0.020	0.990	0.009	0.960	0.953
CM-PAN	0.142	0.049	0.869	0.007	0.854	0.993
AMP-PAN	0.619	0.014	0.994	0.009	0.953	0.989

Cesium breakthrough curve was obtained by plotting the percent of breakthrough C/C_0 versus the number of bed volumes (BV), where C_0 is the initial Cs concentration and C is the C_s concentration in the column effluent. Fig. 8 shows cesium break through curves on synthesized composite ion exchangers. The region where most of the change in concentration occurs is called the mass transfer zone, and the limits are often taken as C/C_0, equal to 0.05–0.95.

To provide an estimate of dynamic capacity, a second order kinetic equation was fit to the data set to obtain a relationship for C_s effluent concentration as function of throughput volume. This equation for C_s concentration was then substituted into the following relationship for dynamic capacity (DC) [43]:

$$DC = \frac{\int_0^{\nu}(C_0 - C)d\nu}{M} \tag{6}$$

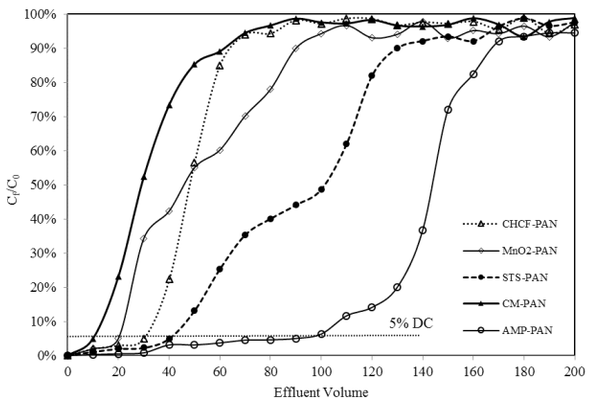

Fig. 8. Breakthrough curves of cesium on the synthesized composite sorbents.

where ν is volume at specified breakthrough, and M is mass of synthesized composite sorbent (*g dry*). Dynamic capacity estimates of the prepared adsorbent were then obtained by evaluating the integral numerically with upper-limit volume values corresponding to approximately 5 and 100% C_s breakthrough. Also, the efficiency of adsorption column (E) was determined by the following formula [21]:

$$E = \frac{A_1}{A_1 + A_2} \times 100 \tag{7}$$

where A_1 is the area above the curve from C/C_0 = 0% till C/C_0= 5%, and A_2 is that from C/C_0 = 5% to C/C_0 = 100%. Adsorption dynamic capacity of the synthesized composite sorbents in 5 and 100% breakthrough conditions, as well as efficiency of the adsorbent column are presented in Table 7.

3.6. Comparison of synthesized composites performance

Table 8 shows a performance comparison of the cesium adsorption by synthesized composite sorbents. The values of K_d, DC-5%and *Efficiency* presented in Table 8, illustrate that AMP-PAN ion exchange performance better than other synthetic absorbents to absorb Cs ions from the solution. Although the structure of synthesized STS-PAN is tunnel-shaped with a high BET value, but it is observed that cesium adsorption rate is lower than synthesized AMP-PAN, which this phenomenon is due to high reluctance of sodium ion contained in the adsorbent structure to interact with cesium ion contained in the solution. Also, because amorphous structure and low BET value,Cs ions adsorption rate by synthesized CM-PAN had the lowest. Therefore the CM-PAN for cesium sorption columns is not recommended as an adsorbent.

Table 7
Adsorption dynamic capacity in dynamic experiment on the synthesized composite sorbents

Composites	Flowrate (BV/h)	Dynamic capacity at 5% breakthrough (Practical)	Dynamic capacity at 100% breakthrough (Total)	Efficiency of adsorbent column (%)
CHCF-PAN	15	7.31 mg Cs/g CHCF-PAN	11.46 mg Cs/g CHCF-PAN	63.78
MnO_2-PAN	15	4.89 mg Cs/g MnO_2-PAN	12.94 mg Cs/g MnO_2-PAN	37.75
STS-PAN	15	9.80 mg Cs/g STS-PAN	22.06 mg Cs/g STS-PAN	44.42
CM-PAN	15	2.43 mg Cs/g CM-PAN	8.5 mg Cs/g CM-PAN	28.67
AMP-PAN	15	21.92 mg Cs/g AMP-PAN	32.34 mg Cs/g AMP-PAN	67.77

Table 8
Performance comparison of the cesium adsorption by the synthesized composite sorbents

Composites	BET (m^2/g)	K_d (mL/g)	Adsorption isotherm	DC-5% (*mg Cs/g adsorbent*)	DC-100% (*mg Cs/g adsorbent*)	*Efficiency*(%)
CHCF-PAN	73.58	1673	Freundlich	7.31	11.46	63.78
MnO_2-PAN	53.03	944	Freundlich	4.89	12.94	37.75
STS-PAN	96.66	2802	Langmuir	9.80	22.06	44.42
CM-PAN	25.18	197	Freundlich	2.43	8.5	28.67
AMP-PAN	75.9	3055	Langmuir	21.92	32.34	67.77

4. Conclusions

In this study, five ion exchangers which include: CHCF-PAN, MnO_2-PAN, STS-PAN, CM-PAN and AMP–PAN were successfully synthesized and compared by various physico-chemical characterization techniques. The studies showed that all of the synthesized composites were thermally stable up to 190ºC and resistant to gamma irradiation of up to 200 KGy. The synthesized composite adsorbents have porous crystalline structure,except for the CM–PAN composite that it had an amorphous structure. As the comparing studies showed, the BET surface area of STS-PAN and AMP-PAN composites wasthe higher than other synthesized composites.

The influence of some parameters, including contact time, solution pH, solution temperature, and interfering cations, were studied on the cesium adsorption by the prepared adsorbent, comprehensively. It was found that pH, temperature, and contact time parameters have increasing effects on the sorption process. On the other hand, the presence of interfering cations had a hindrance effect on the separation of caesium from aqueous solution.

According to adsorption isotherms studies, it can be concluded that the Langmuir model fits the cesium adsorption data on the synthesized AMP-PAN and STS-PAN composites, but adsorption of Cs^+ ions into the CHCF-PAN, MnO_2-PAN and CM-PAN composites correlates well with the Freundlich model. The values of$\Delta H°$,$\Delta S°$and $\Delta G°$ prove that the cesium adsorption on synthesized ion exchangers is an endothermic and spontaneous process.

The overall results indicated that the capability of using the synthesized AMP-PAN and STS-PAN composites for efficient removal of Cs ion from aqueous solutions are more than others synthesized composite adsorbents. It is observed that although the synthesized STS-PAN structure is tunnel-shaped with a high BET value, but cesium adsorption rate is lower than synthesized AMP-PAN, which this phenomenon is due to high reluctance of sodium ion contained in the adsorbent structure to interact with cesium ion contained in the solution. Also, because of amorphous structure and low BET value, the synthesized CM-PAN composite had the lowest Cs ions adsorption rate.

Therefore, it can be concluded that synthesized AMP-PAN composite would be an effective sorbent for the removal of cesium from aqueous solutions, and is recommended as an adsorbent in column separation processes. Calculated dynamic capacities of AMP-PAN for cesium were 21.92 and 32.34 *mg Cs/g sorbent*, for 15 BVs per hour flow at 5 and 100% Cs breakthrough, respectively. In addition, the efficiency of adsorption column was 67.77%.

References

[1] R. Chen, H. Tanaka, T. Kawamoto, M. Asai, C. Fukushima, M. Kurihara, M. Ishizaki, M. Watanabe, M. Arisaka, T. Nankawa, Thermodynamics and mechanism studies on electrochemical removal of cesium ions from aqueous solution using a nano particle film of copper hexacyanoferrate, ACS Appl. Mater. Interfaces, 5 (2013) 12984–12990.

[2] N. Genevios, N. Villandier, V. Chaleix, E. Poil, L. Jauberty, V. Gloaguen, Removal of cesium ion from contaminated water: Improvement of Douglas fir bark biosorption by a combination of nickel hexacyanoferrate impregnation and TEMPO oxidation, Ecol. Eng., 100 (2017) 186–193.

[3] C. Delchet, A. Tokarev, X. Dumail, G. Toquer, Y. Barré, Y. Guari, C. Guerin, J. Larionova, A. Grandjean, Extraction of radioactive cesium using innovative functionalized porous materials, RSC Adv., 2 (2012) 5707–5716.

[4] K. Kubo, K. Nemoto, H. Kobayashi, Y. Kuriyama, H. Harada, H. Matsunami, T. Eguchi, N. Kihou, T. Ota, S. Keitoku, T. Kimura, T. Shinano, Analyses and countermeasures for decreasing radioactivity cesium in buckwheat in areas affected by the nuclear accident in 2011, Field Crop. Res., 170 (2015) 40–46.

[5] H. Rogers, J. Bowers, D. Gates-Anderson, An isotope dilution-precipitation process for removing radioactive cesium from wastewater, J. Hazard. Mater., 243 (2012) 124–129.

[6] M.Y. Miah, K. Volchek, W. Kuang, F.H. Tezel, Kinetic and equilibrium studies of cesium adsorption on ceiling tiles from aqueous solutions, J. Hazard. Mater., 183 (2010) 712–717.

[7] S. Schneider, A.C. Garcez, M. Tremblay, F. Bilodeau, D. Lariviere, F. Kleitz, Nono porous ammonium molybdophosphate-silica hybrids as regenerable ultra-selective extraction agents for radiocesium monitoring, New J. Chem., 37 (2013) 3877–3880.

[8] Y. Park, W. S. Shin, S. J. Choi, Ammonium salt of heteropoly acid immobilized on mesoporous silica (SBA-15): An efficient ion exchanger for cesium ion, Chem. Eng. J., 220 (2013) 204–213.

[9] J. Zheng, W.K. Tagami, Y. Shikamori, K. Nakano, S. Uchida, N. Ishii, Determination of 135Cs and 135Cs/137Cs Atomic Ratio in Environmental samples by combining ammonium molybdophosphate (AMP)-selective Cs adsorption and ion-exchange chromatographic separation to triple-quadrupole inductively coupled plasma-mass spectrometry, Anal. Chem., 86 (2014) 7103–7110.

[10] A. Zhang, E. Kuraoka, M. Kumagai, Group partitioning of minor actinides and rare earths from highly active liquid waste by extraction chromatography utilizing two macro porous silica-based impregnated polymeric composites, Separation and purification technology, 54 (2007)363–372.

[11] A. Zhang, C. Xiao, W. Xue, Z. & Chai, Chromatographic separation of cesium by a macro porous silica-based supra molecular recognition agent impregnated material.,Separ. Purif. Technol., 66 (2009) 541–548.

[12] A. Zhang, E. Kuraoka, M. Kumagai, Impregnation synthesis of a novel macro porous silica-based TODGA polymeric composite and its application in the adsorption of rare earths in nitric acid solution containing diethylenetriaminepentaacetic acid., Eur. Polym. J., 43 (2007) 529–539.

[13] A. Zhang, Y. Wei, H. Hoshi, Y. Koma, M. Kamiya, Partitioning of cesium from a simulated high level liquid waste by extraction chromatography utilizing a macro porous silica-based supramolecular calix [4] arene-crown impregnated polymeric composite,Solv. Extract. Ion Exchange, 25 (2007) 389–405.

[14] A. Zhang, Q. Hu, Z. Chai, SPEC: a new process for strontium and cesium partitioning utilizing two macro porous silica-based supra molecular recognition agents impregnated polymeric composites., Separ. Sci. Technol., 44 (2009) 2146–2168.

[15] H. Deng, Y. Li, Y. Huang, X. Ma, L. Wu, T. Cheng, An efficient composite ion exchanger of silica matrix impregnated with ammonium molybdophosphate for cesium uptake from aqueous solution, Chem. Eng. J., 286 (2016) 25–35.

[16] M. Kapnisti, A.G. Hatzidimitriou, F. Noli, E. Pavlidou, Investigation of cesium uptake from aqueous solutions using new titanium phosphates ion exchangers, J. Radioanal. Nucl. Chem., 302 (2014) 679–688.

[17] Y.K. Kim, Y. Kim, S. Kim, D. Harbottle, J.W. Lee, Solvent-assisted synthesis of potassium copper hexacyanoferrate embedded 3D-interconnected porous hydrogel for highly selective and rapid cesium ion removal, JECE. 5 (2017) 975–986.

[18] H. Deng, Y. Li, L. Wu, X. Ma, The novel composite mechanism of ammonium molybdophosphate loaded on silica matrix and its ion exchange breakthrough curves for cesium, J. Hazard. Mater., 324 (2016) 348–356.

[19] A.M. El-Kamash, Evaluation of zeolite A for the sorptive removal of Cs^+ and Sr^{2+} ions from aqueous solutions using batch and fixed bed column operations, J. Hazard. Mater., 151 (2008) 432–445.

[20] A. Nilchi, R. Saberi, M. Moradi, H. Azizpour, R. Zarghami, Adsorption of cesium on copper hexacyanoferrate–PAN composite ion exchanger from aqueous solution, Chem. Eng. J., 172 (2011) 572–580.
[21] C.S. Griffih, V. Luca, J.V. Hanna, K.J. Pike, M.E. Smith, G.S. Thorogood, Micro crystalline hexagonal tungsten bronze. 1. Basis of ion exchange selectivity for cesium and strontium, Inorg. Chem., 48 (2009) 5648–5662.
[22] B. Bartoś, B. Filipowicz, M. Lyczko, A. Bilewicz, Adsorption of ^{137}Cs on titanium ferrocyanide and transformation of the sorbent to lithium titanate: a new method for long term immobilization of 137Cs, J. Radioananl. Nucl. Chem., 302 (2014) 513–516.
[23] H.M. Liu, A. Yonezawa, K. Kumagai, M. Sano, T. Miyake, Cs and Sr removal over highly effective adsorbents ETS-1 and ETS-2, J. Mater. Chem., A. 3 (2015) 1562–1568.
[24] D. Sarma, C.D. Malliakas, K.S. Subrahmanyam, S.M. Islama, M.G. Kanatzidis, $K_{2x}Sn_{4-x}S_{8-x}$(x=0.65–1): a new metal sulfide for rapid and selective removal of Cs^+, Sr^{2+} and UO_2^{2+} ions, Chem. Sci., 7 (2016) 1121–1132.
[25] S.B. Yang, N. Okada, M. Nagatsu, The highly effective removal of Cs^+ by low turbidity chitosan-grafted magnetic bentonite, J. Hazard. Mater., 301 (2016) 8–16.
[26] R. Saberi, A. Nilchi, S. Rasouli Garmarodi, R. Zarghami, Adsorption characteristic of ^{137}Cs from aqueous solution using PAN-based sodium titanosilicate composite, J. Radioanal. Nucl. Chem., 284 (2010) 461–469.
[27] A. K. Kaygun and S. Akyil, Study of the behaviour of thorium adsorption on PAN/zeolite composite adsorbent, J. Hazard. Mater. 147 (2007) 357-362.
[28] F. Sebesta, J. John, A. Motl, J. Watson, Development of PAN-based adsorbers for treating waste problems at U.S. DOE facilities, In: S. Slate, F. Feizollahi and J. Creer., Eds., ICEM. 1 (1995) 361–370.
[29] A. Nilchi, A. Khanchi, H. Atashi, A. Bagheri, L. Nematollahi, The application and properties of composite sorbents of inorganic ion exchangers and polyacrylonitrile binding matrix, J. Hazard. Mater., 137 (2006) 1271–1276.
[30] H.H. Someda, A.A. El-Zahhar , M.K. Shehata, H.A. El-Naggar , Supporting of some ferrocyanides on polyacrylonitrile (PAN) binding polymer and their application for cesium treatment, Sep. Purif. Technol., 29 (2002) 53–61.
[31] S. Milonji, I. Bispo, M. Fedoroff, C. Loos-Neskovicv, C. Vidal-Madjar, Sorption of cesium on copper hexacyanoferrate/polymer/silica composites in batch and dynamic conditions, J. Radioananl. Nucl. Chem., 252 (2002) 497–501.
[32] C. Sun, F. Zhang, X. Wang, F. Cheng, Facile preparation of ammonium molybdophosphate/Al-MCM-41 composite material from natural clay and its use in cesium ion adsorption, European J. Inorg. Chem., 12 (2015) 2125–2131.
[33] A. Nilchi, R. Saberi, S. RasouliGarmarodi, A. Bagheri, Evaluation of PAN-based manganese dioxide composite for the sorptive removal of cesium-137 from aqueous solutions, App. Rad. Isotop., 70 (2012) 369–374.
[34] A. Nilchi , R. Saberi, H. Azizpour, M. Moradi, R. Zarghami, M. Naushad, Adsorption of caesium from aqueous solution using cerium molybdate–pan composite, Chem. Eco. 28 (2011) 1–17.
[35] A. Nilchi, R. Saberi, M. Moradi, H. Azizpour, Evaluation of AMP–PAN composite for adsorption of Cs^+ ions from aqueous solution using batch and fixed bed operations, J. Radioananl. Nucl. Chem., 292 (2011) 609–617.
[36] J.K. Moon, K.W. Kim, C.H. Jung, Y.G. Shul, E.H. Lee, Preparation of organic-inorganic composite adsorbent beads for removal of radio nuclides and heavy metal ions, J. Radioananl. Nucl. Chem., 246 (2000) 299–307.
[37] A. Nilchi, M.R. Hadjmohammadi, S. Rasouli Garmarodi, R. Saberi, Studies on the adsorption behavior of trace amounts of $^{90}Sr^{2+}$, $^{140}La^{3+}$, $^{60}Co^{2+}$, $Ni^{2+}$and Zr^{4+} cations on synthesized inorganic ion exchangers, J. Hazard. Mater., 167 (2009) 531–535.
[38] A.J. Celestian, D.G. Medvedev, A. Tripathi, J.B. Parise, A. Clearfield, Optimizing synthesis of $Na_2Ti_2SiO_7.2H_2O$ (Na-CST) and ion exchange pathways for $Cs_{0.4}H_{1.6}Ti_2SiO_7.H_2O$ (Cs-CST) determined from in situ synchrotron X-ray powder diffraction, Nucl. Inst. Meth. Phys. Res. Sec. B., 238 (2005) 61–69.
[39] J.D. Hanawalt, Powder diffraction file search manual (Hanawalt method) Inorganic, Swarthmore, PA., ICDD. (1986) 12–716.
[40] A. Nilchi, H. Atashi, A. H. Javid, R. Saberi, Preparations of PAN-based adsorbers for separation of cesium and cobalt from radioactive wastes, Appl. Rad. Isotop., 65 (2007) 482–487.
[41] V. Moraes, B. Marczewski, C.R. Dias, J.A. Junior, Study of gels of molybdenum with cerium in the preparation of generators of ^{99}Mo - ^{99m}Tc, BABT. 48 (2005) 51–56.
[42] Y. Park, Y.C. Lee, W.S. Shin, S.J. Choi, Removal of cobalt, strontium and cesium from radioactive laundry wastewater by ammonium molybdophosphate–polyacrylonitrile (AMP–PAN), Chem. Eng. J., 162 (2010) 685–695.
[43] J. Wu, B. Li, J. Liao, Y. Feng, D. Zhang, J. Zhao, W. Wen, Y. Yang, N. Liu, Behavior and analysis of Cesium adsorption on montmorillonite mineral, J. Environm. Rad., 100 (2009) 914–920.
[44] R. Cortés-Martínez, M.T. Olguín, M. Solache-Ríos, Cesium sorption by clinoptilolite-rich tuffs in batch and fixed-bed systems, Desalination, 258 (2010) 164–170.
[45] M. Prasad, H.Y. Xu, S. Saxena, Multi-component sorption of Pb (II), Cu (II) and Zn (II) onto low-cost mineral adsorbent, J. Hazard. Mater., 154 (2008) 221–229.
[46] I. Langmuir, The constitution and fundamental properties of solids and liquids, JACS. 38 (1916) 2221–2295.
[47] H.M. Freundlich, Uber die adsorption in losungen, Zeitschrift fur PhysikalischeChemie., 57 (1906) 385–470.
[48] T.A. Todd, V.N. Romanovskiy, A Comparison of Crystalline Silicotitanate and Ammonium Molybdophosphate-Polyacrylonitrile Composite Sorbent for the Separation of Cesium from Acidic Waste, Radiochemistry, 47 (2005) 398–402.